# Accepted Manuscript


Development of cell-penetrating asymmetric interfering RNA targeting connective tissue growth factor (CTGF)

Jihye Hwang, Chanil Chang, Ji Hyun Kim, Chang Taek Oh, Ha Neul Lee, Changki Lee, Donghoon Oh, Changjin Lee, Beomjoon Kim, Sun Woo Hong, Dong-ki Lee

PII: S0022-202X(16)32106-6

DOI: 10.1016/j.jid.2016.06.626

Reference: JID 443

To appear in: *The Journal of Investigative Dermatology*

Received Date: 16 December 2015

Revised Date: 10 June 2016

Accepted Date: 16 June 2016

Please cite this article as: Hwang J, Chang C, Kim JH, Oh CT, Lee HN, Lee C, Oh D, Lee C, Kim B, Hong SW, Lee D-k, Development of cell-penetrating asymmetric interfering RNA targeting connective tissue growth factor (CTGF), *The Journal of Investigative Dermatology* (2016), doi: 10.1016/j.jid.2016.06.626.

# Development of cell-penetrating asymmetric interfering RNA targeting connective tissue growth factor (CTGF)

**Jihye Hwang[1], Chanil Chang[1], Ji Hyun Kim[1], Chang Taek Oh[2], Ha Neul Lee[3], Changki Lee[3], Donghoon Oh[3], Changjin Lee[3], Beomjoon Kim[2], Sun Woo Hong[1], and Dong-ki Lee[4]**

[1]OliX Pharmaceuticals, Inc., Seoul, Korea, [2]Department of Dermatology, Chung Ang University Medical Center, Seoul, Korea, [3]Hugel Inc., Chuncheon, Korea, [4]Department of Chemistry, Sungkyunkwan University, Suwon, Korea

**City and country in which the work was done**: Seoul, Chuncheon and Suwon, Korea.

**Correspondence:** Dong-ki Lee, Department of Chemistry, Sungkyunkwan University, Suwon, Korea, 440-746. Tel: (+82)31-299-4565, Fax: (+82)31-299-4890, Email: dklee@skku.edu.

**Short title:** Development of RNAi compounds targeting CTGF

**Abbreviations**

**cp-asiRNA:** cell-penetrating asymmetric RNAi triggers

**MTS:** Masson's trichrome staining

**ABSTRACT**

Connective tissue growth factor (CTGF) is a multifunctional matricelluar protein, playing a role as a central mediator in tissue remodeling and fibrosis. A number of reports have demonstrated the pivotal roles of CTGF in the progression of fibrosis, suggesting CTGF as a promising therapeutic target for the treatment of fibrotic disorders including hypertrophic scars and keloids. In this study, we present the development of a interfering RNA molecule which efficiently inhibits the expression of CTGF via RNA interference mechanism both *in vitro* and *in vivo*. Chemical modifications were introduced to the asymmetric interfering RNA (asiRNA) backbone structure. The resulting RNA molecule, termed cell-penetrating asiRNA (cp-asiRNA), entered into cells and triggered RNAi-mediated gene silencing without delivery vehicles. The gene silencing activity of cp-asiRNA targeting CTGF (cp-asiCTGF) was examined both *in vitro* and *in vivo*. Furthermore, the administration of cp-asiCTGF in the rat skin excision wound model efficiently reduced the induction of CTGF as well as collagens during the wound healing process. These result suggest that the cp-asiCTGF molecule could be developed into anti-fibrotic therapeutics such as anti-scar drugs.

## INTRODUCTION

Connective tissue growth factor (CTGF/CCN2) is a secreted matricellular protein known to play important roles in many biological processes, including cell adhesion, migration, proliferation, angiogenesis, vascular differentiation and myofibroblast formation, all of which can lead to tissue remodeling and changes in organ structure.(Lipson et al., 2012) . One of the key functions of CTGF is controlling and coordinating signal transduction pathways involving cell surface proteoglycans, which are components of the extracellular matrix and growth factors. Over-expression of CTGF is known to be associated with the pathology of a number of fibrotic disorders such as skin fibrosis (hypertrophic scar and keloid), fibrotic liver disease, idiopathic pulmonary fibrosis, proliferative diabetic retinopathy, and diabetic kidney disease.(Gressner and Gressner, 2008; Ihn, 2002; Kono et al., 2011; Rachfal and Brigstock, 2003)

In skin, collagen is the major structural protein and CTGF functions as an intrinsic, physiological mediator of collagen type I & III expression. During the wound healing process, transforming growth factor-β (TGF-β) stimulates the expression of CTGF and induces CTGF-triggered collagen production.(Colwell et al., 2005) Thus, CTGF is suggested as an important target for the treatment of hypertrophic scars and keloids, which are caused by excessive fibrosis during the wound healing process. Indeed, several studies confirmed that the inhibition of CTGF expression or activity by antisense oligonucleotides or antibodies lead to a reduction in excessive collagen deposition and the pathologic severity of fibrosis.(Sisco et al., 2008; Wang et al., 2011)

RNA interference (RNAi) is a highly specific and efficient mechanism of eukaryotic gene

suppression, which is mediated by a short double-stranded RNA termed small interfering RNA (siRNA). Intracellular delivery of siRNA leads to the inhibition of target gene expression via specific recognition and cleavage of mRNA with sequence complementarity to siRNA, catalyzed by the cellular RNAi machinery. Due to the unparalleled specificity and efficiency in target gene silencing, RNAi-mediated gene silencing is regarded as one of the most promising therapeutic development platforms against various diseases.(Carthew and Sontheimer, 2009; Dorsett and Tuschl, 2004; Elbashir et al., 2001)

Despite high expectations, efficient delivery of siRNA molecules to diseased tissue or organs *in vivo* still remains a major obstacle to be overcome in the development of effective RNAi therapeutics. The highly negative charges of siRNA due to the phosphate backbone structure prevent siRNA from entering the cell through the plasma membrane. Therefore, it is necessary to use delivery vehicles, e.g. liposomes and nanoparticles, in order to achieve the proper tissue distribution and cellular uptake of siRNA.

Instead of using delivery vehicles, direct introduction of chemical modifications to the siRNA backbone was also attempted to improve cellular uptake. For example, several studies reported that conjugation of a cholesterol moiety to the siRNA enables the intracellular uptake of siRNA.(Soutschek et al., 2004; Wolfrum et al., 2007) In addition to its role in protecting against nuclease activity, phosphorothioate modification was reported to enhance intracellular delivery of oligonucleotides.(Connolly et al., 1984; Spitzer and Eckstein, 1988; Thierry and Dritschilo, 1992; Woolf et al., 1990; Zhao et al., 1993) Accordingly, these findings suggest that it is possible to

develop potent RNAi therapeutics by introducing optimal chemical modifications to the siRNA molecule.

In this study, we present the successful development of a potent RNAi triggering molecule targeting CTGF. Previously, we introduced a siRNA structure termed asymmetric siRNA (asiRNA), which had significantly mitigated off-target effects compared to conventional siRNA. (Chang et al., 2009; Hong et al., 2014; Jo et al., 2011) Based on the asiRNA backbone structure, we introduced several chemical modifications, such as cholesterol conjugation and phosphorothioate, to enhance the intracellular uptake of the RNAi triggering molecule. We also incorporated 2'-O-methyl (2'OMe) to enhance the stability of the asiRNA. The resulting RNAi trigger targeting CTGF (cp-asiCTGF) showed efficient target gene suppression activity without the need for delivery vehicles both *in vitro* and *in vivo*.

## RESULTS

### Selection of a potent cp-asiRNA targeting CTGF (cp-asiCTGF)

In order to identify effective asiRNA candidates with the most potent target gene silencing effects, 40 target sequences spanning the length of the human CTGF mRNA were chosen and the corresponding asiRNAs were designed for each sequence. Based on the CTGF repression activity, asiRNA with the most potent target gene silencing activity were selected (data not shown). Then, chemical modifications were introduced to the selected asiRNAs to generate cell penetrating asiRNAs (cp-asiRNAs). The resulting cp-asiRNA targeting CTGF (cp-asiCTGF, Figure 1a) carries chemical modifications such as cholesterol conjugation at the 3'-end of the passenger strand, phosphorothioate backbone modification, and 2'-O-Methyl modification of the ribose sugar on both strands.

### Inhibition of CTGF expression by cp-asiCTGF *in vitro*

Target gene silencing activity for cp-asiCTGF was analyzed in the human lung adenocarcinoma A549 cells which express target gene CTGF. As shown in Fig. 1b, the transfection of CTGF-targeting RNAi triggering molecules including conventional siRNA (siCTGF), asiRNA (asiCTGF), and asiRNA with chemical modification described in Fig. 1a (cp-asiCTGF) efficiently reduced the target gene expression at the mRNA level. In detail, we observed that cp-asiCTGF has most potent target gene silencing activity between tested RNAi triggering molecules. At the concentrations tested (50 nM final), more than 85% knock-down by cp-asiCTGF was observed (Fig. 1b). Then, we investigated the target gene silencing activity of cp-asiCTGF without the aid of a transfection reagent. A549 cells were treated with media containing

siCTGF, asiCTGF, or cp-asiCTGF, and the target gene level was analyzed. We observed potent target mRNA repression by cp-asiCTGF (Fig. 1b). The incubation of cells with 1 μM cp-asiCTGF resulted in more than 85% knock-down of CTGF at the mRNA level. On the other hand, neither siCTGF or asiCTGF treated sample showed significant target mRNA reduction without the aid of delivering reagent. For dose response analysis, A549 cells were treated with media containing different concentrations of cp-asiCTGF and dose dependent target mRNA knockdown by cp-asiCTGF was confirmed ($IC_{50}$ = 0.315 nM, Fig. 1c).

CTGF protein level knockdown analysis was conducted under the condition of transforming growth factor β (TGF-β) induction. CTGF mRNA in A549 cells is detectable in northern blot analysis in previous study (Hishikawa et al., 1999a) and we also observed modest expression of CTGF mRNA level in the present study. In detail, real-time PCR raw data reported cycle threshold ($C_T$) value for CTGF was about 26.5. However, CTGF protein is known to merely detectable in A549 cell lysate (Chang et al., 2004) attributed from the nature of the protein as a secreted protein. TGF-β treatment is known to induce expression of CTGF (Hishikawa et al., 1999b; Hishikawa et al., 1999c) and we observed induction of CTGF mRNA and protein expression in the presence of TGF-β in A549 cells (Figure 2a, b). In this condition, cp-asiCTGF treatment reduced the expression of the target mRNA and protein as well in a dose-dependent manner (Figure 2a, b). Efficient reduction of CTGF mRNA and protein level by cp-asiCTGF was observed in other cell lines such as HaCaT and HeLa cells (Figure 2a, b). Furthermore, target gene silencing by cp-asiCTGF was examined in keloid fibroblast KEL FIB cells. A previous study reported high expression of CTGF in the keloid tissue extract, consistent with the idea that CTGF plays an important role in keloid pathogenesis by promoting collagen synthesis and

deposition (Khoo et al., 2006). Thus, it is expected that potent RNAi triggers targeting CTGF could be developed as therapeutics for keloid treatment. We observed high basal level expression of CTGF in the KEL FIB cells, which was efficiently reduced by cp-asiCTGF treatment (Figure 2c).

***In vivo* examination of cp-asiCTGF target gene silencing activity**

As the next step, *in vivo* analysis of cp-asiCTGF was conducted. Several studies describe target gene knockdown by intradermal injection of oligonucleotides without aid of delivering reagents in rat skin (Sisco et al., 2008; Karen et al, 2014). In addition to the animal studies, dose range from sub-milligram to milligrams per injection was suggested from human clinical trials design (NCT02030275 and NCT01037985). We examined target gene silencing by cp-asiCTGF intradermal injection with different doses in rat skin. Four different amount of cp-asiCTGF ranging from 0.1 to 1 mg were injected into rat skin and, after 24 hours, skin biopsy samples were collected from the injection sites and subjected to qRT-PCR analysis in order to assess the mRNA level of CTGF. The analysis showed that the intradermal injection of cp-asiCTGF led to potent target gene silencing in dose dependent manner (Figure 3a). On the other hand, SC cp-asiCTGF (cp-asiRNA with a scrambled sequence used as the negative control) did not reduce CTGF mRNA level at 1 mg injection condition (Figure 3a). The specific knockdown by cp-asiCTGF was also confirmed in target protein analysis after 72 hours of intradermal injection. As shown in Figure 3b, significant reduction of CTGF protein was observed in cp-asiCTGF-treated samples compared to the scrambled cp-asiRNA-treated samples (SC cp-asiCTGF). To visualize cp-asiCTGF distribution after intradermal injection, rat skin was intradermally injected with Cy5.5-labeled cp-asiCTGF, and its distribution was analyzed by laser confocal scanning microscopy.

The result showed extensive distribution of fluorescent signals at the site of injection (Figure 3c), suggesting the efficient delivery of cp-asiRNA into cells, followed by potent target gene silencing *in vivo*. We also compared *in vivo* target gene silencing activity of cp-asiCTGF with commercially available self-delivery siRNA (Figure S1). The results showed that the cp-asiCTGF have higher target gene silencing potency than the commercially available siRNA in both mRNA and protein level. In detail, compared to the commercially available siRNA, cp-asiCTGF showed similar or higher level of target gene knockdown in 10-fold lower dose.

**Effect of cp-asiCTGF on rat skin excision wound model**

We further investigated the *in vivo* effects of cp-asiCTGF in the rat skin excision wound model. Consistent with its key roles in fibrosis, CTGF is known to be up-regulated at wound sites in the excision wound model (Mori et al., 2002; Sisco et al., 2008). After the establishment of excision wounds (Day 0), cp-asiCTGF or SC cp-asiCTGF was treated via intradermal injection on Days 14, 18, 22 and 26. On Day 29, skin samples were collected and subjected to further analysis. We exploited qRT-PCR analysis to measure CTGF mRNA and western blot and immunohistochemistry analysis to measure CTGF protein. At the time of harvest, the level of CTGF mRNA in the cp-asiCTGF treated samples was reduced by about 80% in comparison to saline treated samples while the SC cp-asiCTGF did not show any effect on the level of CTGF mRNA (Figure 4a). We also examined the expression of rat collagen type I and III at the mRNA level. Consistent with the change in CTGF mRNA, the levels of collagen type I and III mRNA were also reduced in cp-asiCTGF treated samples (Figure 4b, c). Similar to the mRNA level, western blot analysis also confirmed potent target gene silencing activity of cp-asiCTGF while the administration of the SC cp-asiCTGF did not affect CTGF and collagen type I protein level

(Figure 4d, e).

The decrease in CTGF and collagen type I proteins was also observed by immunohistochemistry analysis in tissue sections of skin treated with cp-asiCTGF (Figure 5a, b, c, d, e and f). As shown in figure 5a and 5b, intradermal injection of cp-asiCTGF resulted in a reduction in CTGF protein staining in comparison to the saline treated control in the dermis at the wound sites. Injection of SC cp-asiCTGF, however, was not resulted in target protein reduction (Figure 5c and j). Immunohistochemistry analysis for collagen type I also demonstrated effective reduction of the collagen type I level by cp-asiCTGF administration at the dermis (Figure 5d, e, f and k). In addition, the sectioned skin samples were stained with Masson's Trichrome staining (MTS) to confirm the collagen levels in excision wound skin (Figure 5g, h and i). In saline treated samples, markedly increased collagen deposition at the excision site was observed compared to surrounding normal tissue (Figure 5g). In contrast, cp-asiCTGF treated skin showed a reduced level of collagen at the excision site while the control siRNA (SC cp-asiCTGF) did not affect level of collagen (Figure 5g, h, i and l).

## DISCUSSION

In this study, we developed cp-asiRNA, an RNAi trigger platform with cell membrane penetrating capability. This RNAi trigger is structurally based on asymmetric siRNA with a shortened passenger strand (16 nt), which shows reduced nonspecific effects compared to conventional siRNA (Chang et al., 2009; Hong et al., 2014; Jo et al., 2011). In addition, cp-asiRNA has chemical modifications including cholesterol conjugation, phosphorothioate (PS) modification and 2'-O-metyl (2'-OMe) modification. PS modification is known to increase endocytosis as well as to improve serum stability (Ge et al., 2010). Nucleic acids conjugated with cholesterol interact with the membranes of cells and enhance cellular uptake (Soutschek et al., 2004; Wolfrum et al., 2007). 2'-OMe modification to RNA has been shown to increase siRNA stability against endonucleases and reduce immune stimulation (Burnett and Rossi, 2012). We confirmed that the cp-asiRNA harboring these modifications exhibited potent target gene silencing ability without the aid of delivery vehicles, suggesting that the cp-asiRNA is a potent RNAi trigger compound that can be developed for RNAi therapeutics.

Using the cp-asiRNA targeting CTGF, we showed efficient *in vitro* and *in vivo* target gene silencing. We also examined the effect of cp-asiCTGF treatment in a rat skin excision wound model and the results demonstrated potent CTGF gene silencing along with a reduced level of fibrosis. We expect that the cp-asiCTGF compound has great potential to be further developed into therapeutics for treating skin fibrotic disorders including hypertrophic scars and keloids.

## MATERIALS AND METHODS

### siRNAs

Chemically synthesized, high-performance liquid chromatography-purified RNAs were purchased from STpharm (Seoul, South Korea) and annealed according to the manufacturer's instructions. Sequence information for each RNA is provided in Table S1.

### Transfection and treatment of siRNAs

A549, HaCaT, HeLa and KEL FIB cells were purchased from ATCC and maintained at 37 ºC in Dulbecco's modified Eagle's medium (Invitrogen, Calsbad, CA) supplemented with 10% (v/v) fetal bovine serum, 100 U/ml penicillin, and 100 μg/ml streptomycin. Cells were routinely subcultured to maintain exponential growth. For transfection, cells were plated on 12-well plates 24 hours before transfection at 30%-50% confluence in complete medium. Lipofectamine 2000 was used for transfection following the manufacturer's protocol (Invitrogen). Cells were harvested 24 hours after transfection for further analysis. For the treatment of siRNAs without transfection reagent, cells were plated in 12-well plates at 30-50% confluence in complete medium. After 24 hours, cells were washed with 1xDPBS (Gibco) and incubated for 4 hours in Opti-MEM containing siRNA. Then the siRNA-containing Opti-MEM media was replaced with serum containing complete media. After 24 hours or 48 hours, further analysis was conducted including target gene expression analysis. For TGF-β induction, cells were treated with 2ng/ml TGF-β (R&D Systems, Minneapolis, MN) in serum containing complete media for 24hours.

### Quantitative real-time polymerase chain reaction

Total RNA were extracted using RNAiPlus® (TaKaRa) and then 0.5 μg of total RNA was used for cDNA synthesis using the High-capacity cDNA reverse transcription kit (Applied Biosystems)

according the manufacturer's protocol. Aliquots (1/20) of each cDNA reaction were analyzed by quantitative real-time reverse transcription–polymerase chain reaction (qRT-PCR) using the StepOne Real-Time PCR System (Applied Biosystems). Gene-specific primers were mixed with SYBR green PCR master Mix (Applied Biosystems). In the analysis of the siRNA target gene knock-down efficiency, the target genes and internal control mRNA levels were determined using the relative standard curve quantitation method. The primer sequences for each gene are shown below:

Human GAPDH-forward: 5'-GAGTCAACGGATTTGGTCGT-3'

Human GAPDH-reverse: 5'-GACAAGCTTCCCGTTCTCAG-3'

Human CTGF-forward: 5'-CAAGGGCCTCTTCTGTGACT-3'

Human CTGF-reverse: 5'-CCGTCGGTACATACTCCACA-3'

Rat GAPDH-forward: 5'-AGACAGCCGCATCTTCTTGT-3'

Rat GAPDH-reverse: 5'-CTTGCCGTGGGTAGAGTCAT-3'

Rat CTGF-forward: 5'-CGGGAAATGCTGTGAGGAGT-3'

Rat CTGF-reverse: 5'-GGCTCGCATCATAGTTGGGT-3'

Rat Collagen type I-forward: 5'-AGCGTGCTGTAGGTGAATCG-3'

Rat Collagen type I-reverse: 5'-AACCCCAAGGAGAAAAAGCA-3'

Rat Collagen type III-forward: 5'-TGCATAAATGCCAGTCCCAT-3'

Rat Collagen type III-reverse: 5'-GGCAATGCTGTTTTTGCAGT-3'

**Western blot analysis**

Total proteins were extracted using Mammalian protein Extraction Buffer (GE Healthcare) and protease inhibitor cocktail (Roche). The protein concentration was measured using a Bradford assay kit. Equal amounts of protein were resolved via SDS-PAGE gel electrophoresis. After electrophoresis, the proteins were transferred to PVDF membrane (Bio-rad) already activated by methanol (Merck) for 1 hour. The membrane was blocked for 1 hour at room temperature with 5% skim milk and then incubated overnight at 4 ºC in 5% skim milk containing specific antibodies (Anti-CTGF antibody: Novus and Santa cruz, anti-β-Actin antibody: Santa cruz, anti-GAPDH antibody: Santa cruz, anti-HSP90 antibody: Novus). The membrane was washed with Tris-buffered saline containing 1% Tween-20 and incubated for 1 hour at room temperature in 5% skim milk with HRP-conjugated secondary antibody (Santa cruz). After incubation, the membrane was treated with ECL substrate (Thermo scientific). The target protein bands were then imaged using a Chemidoc instrument (Bio-rad). The western blot bands were quantified by densitometry using the ImageJ software and CTGF protein expression was normalized by loading control expression.

***In vivo* study**

All animal studies were performed in compliance with the policies of the Sungkyunkwan University Animal Care and Use Committee. SD rats (males, 6-8weeks old) were purchased from Orient Bio (Korea). The rats were anaesthetized prior to cp-asiCTGF treatment with 30 mg/kg of intramuscular Zoletil and 10 mg/kg of intramuscular Rompun. A total dose of 0.1, 0.4, 0.7, or 1 mg of siRNA dissolved in saline solution per injection was administered in a total volume of 100 μl (from a stock solution of 10 mg/ml). For mRNA level analysis, injection site skin at 24 hours after treatment was isolated and subjected to qRT-PCR. For protein level analysis, injection site skin at 72 hours after treatment was isolated and subjected to western blot analysis.

**Rat excision wound model study**

The rats were anaesthetized prior to creation of the wounds or with 30 mg/kg of intramuscular Zoletil and 10 mg/kg of intramuscular Rompun. The dorsal skin was punctured to create an excision wound with a width of 8 mm (circular area = 50 $mm^2$) using a disposable biopsy punch. 14 days after treatment, the subjects were divided into three groups (n = 5). Group 1 animals were injected with saline (vehicle only control). Group 2 animals were injected with cp-asiCTGF and Group 3 animals were injected with SC cp-asiCTGF (cp-asiRNA with a scrambled sequence used as the negative control) every 4 days. Total dose of 1.5 mg of siRNA in dissolved in 150 μl saline solution was administered. In detail, 50 μl volume of each siRNA containing solution was injected intradermally at three different positions around excision site. The skin was injected 4 times (Day 14, 18, 22, and 26) and analyzed 29 days after initial excision wound treatment.

**Confocal microscopy analysis of fluorescent labeled cp-asiRNA**

Cy5.5 labeled cp-asiRNA was administered to rat skin by intradermal injection. The skin from the biopsy was embedded in O.C.T compound (Tissue-Tek, Torrance, CA) and frozen in dry ice. Vertical cross sections (20 μm) were prepared and stained with 4,6-diamidino-2-phenylindole (Sigma). After DAPI staining, the tissue was mounted with Fluorescence Mounting Media (Dacko). Tissue sections were imaged with a red fluorescent filter set in Leica TCS SP8. To increase the effective resolution of the Fluorescence image, 5 images were taken at each z-step, and these 5 image sets were averaged to produce z-step-averaged images, resulting in the final image stack.

**Immunohistochemistry and Masson's Trichrome staining**

An immunohistochemistry accessory kit (Bethyl laboratories, Inc., Montgomery, TX) was used to

examine the expression levels of CTGF and Collagen type I according to the manufacturer's instructions. Briefly, after deparaffinization and rehydration, the slides were incubated in 3% hydrogen peroxide/methanol to quench endogenous peroxidase. Slides were then incubated in hot Epitope retrieval buffer (provided in kit) to recover epitopes for 20 min at 98°C. Non-specific reactions were blocked by incubating the sections with blocking reagent (included in the kit) for 30 min at room temperature, then 100 µl of CTGF antibody (dilution 1:100, anti-rabbit, Novus) or 100 µl of collagen type I antibody (dilution 1:100, anti-rabbit, Thermo scientific) was applied to each slide and incubated overnight at 4°C. Slides were then incubated with working anti-rabbit IHC antibody (provided in kit), and peroxidase activity was visualized with working 3, 3′-diaminobenzidine (DAB) substrate (provided in kit). Counterstaining was performed with hematoxylin. Quantitative analysis of stained sections was performed using Image Gauge 4.0 (Fuji Photo Film co., Tokyo, Japan). In this study, immune-positive areas were measured in each region of interest (ROI) using a grid and their proportion among the total stained section was analyzed.

Skin tissue sections were obtained and stained with Masson’s Trichrome Stain (MTS) and toluidine blue by KCFC pathology laboratory (Korea, Seoul). The slides stained with Masson’s trichrome stain were examined using slide scanner and with the aid of ImageJ software, measurements were made at the intensity of blue color which represent the collage density. Collagen density was measured under the wound area compared to normal dermis. For each group, the mean of the collagen density under wound area was expressed in the ratio of percentage compared to collagen density of normal dermis (Suvik and Effendy, 2012).

**Statistical analysis**

Statistical significance was assessed by Student’s t-test.

## CONFLICT OF INTEREST

The intellectual property relating to this study is owned by OliX pharmaceuticals, Inc.

## ACKNOWLEDGEMENT

This work was supported by the Korea Drug Development Fund (KDDF-201408-14) funded by Ministry of Science, ICT and Future Planning, Ministry of Trade, Industry & Energy and Ministry of Health & Welfare and the Technological Innovation R&D Program (S2090744) funded by the Small and Medium Business Administration (SMBA, Korea).

**REFERENCES**

Burnett JC, Rossi JJ. RNA-based therapeutics: current progress and future prospects. Chem Biol 2012;19:60-71.

Carthew RW, Sontheimer EJ. Origins and Mechanisms of miRNAs and siRNAs. Cell 2009;136:642-55.

Chang CC, Shih JY, Jeng YM, Su JL, Lin BZ, Chen ST, et al. Connective tissue growth factor and its role in lung adenocarcinoma invasion and metastasis. J Natl Cancer Inst 2004;96:364-75.

Chang CI, Yoo JW, Hong SW, Lee SE, Kang HS, Sun X, et al. Asymmetric shorter-duplex siRNA structures trigger efficient gene silencing with reduced nonspecific effects. Mol Ther 2009;17:725-32.

Colwell AS, Phan TT, Kong W, Longaker MT, Lorenz PH. Hypertrophic scar fibroblasts have increased connective tissue growth factor expression after transforming growth factor-beta stimulation. Plast Reconstr Surg 2005;116:1387-90; discussion 91-92.

Connolly BA, Potter BV, Eckstein F, Pingoud A, Grotjahn L. Synthesis and characterization of an octanucleotide containing the EcoRI recognition sequence with a phosphorothioate group at the

cleavage site. Biochemistry 1984;23:3443-53.

Dorsett Y, Tuschl T. siRNAs: applications in functional genomics and potential as therapeutics. Nat Rev Drug Discov 2004;3:318-29.

Elbashir SM, Harborth J, Lendeckel W, Yalcin A, Weber K, Tuschl T. Duplexes of 21-nucleotide RNAs mediate RNA interference in cultured mammalian cells. Nature 2001;411:494-8.

Ge Q, Dallas A, Ilves H, Shorenstein J, Behlke MA, Johnston B. Effects of chemical modification on the potency, serum stability, and immunostimulatory properties of short shRNAs. Rna 2010;16:118-30.

Gressner OA, Gressner AM. Connective tissue growth factor: a fibrogenic master switch in fibrotic liver diseases. Liver Int 2008;28:1065-79.

Hishikawa K, Oemar BS, Tanner FC, Nakaki T, Luscher TF, Fujii T. Connective tissue growth factor induces apoptosis in human breast cancer cell line MCF-7. J Biol Chem 1999a;274:37461-66.

Hishikawa K, Nakaki T, Fujii T. Transforming growth factor-beta(1) induces apoptosis via

connective tissue growth factor in human aortic smooth muscle cells. Eur J Pharmacol 1999b;385:287-90.

Hishikawa K, Oemar BS, Tanner FC, Nakaki T, Fujii T, Luscher TF. Overexpression of connective tissue growth factor gene induces apoptosis in human aortic smooth muscle cells. Circulation 1999c;100:2108-12.

Hong SW, Park JH, Yun S, Lee CH, Shin C, Lee DK. Effect of the guide strand 3'-end structure on the gene-silencing potency of asymmetric siRNA. Biochem J 2014;461:427-34.

Ihn H. Pathogenesis of fibrosis: role of TGF-beta and CTGF. Curr Opin Rheumatol 2002;14:681-85.

Jo SG, Hong SW, Yoo JW, Lee CH, Kim S, Kim S, et al. Selection and optimization of asymmetric siRNA targeting the human c-MET gene. Mol Cells 2011;32:543-48.

Karen B, James C, Katherine H, Lakshmipathi P, Lyn L, Michael B. Reduction of connective tissue growth factor by an RNA interference mechanism as a potential treatment for fibrotic skin indications. J Am Acad Dermatol 2014;70:AB196.

Khoo YT, Ong CT, Mukhopadhyay A, Han HC, Do DV, Lim IJ, et al. Upregulation of secretory connective tissue growth factor (CTGF) in keratinocyte-fibroblast coculture contributes to keloid pathogenesis. J Cell Physiol 2006;208:336-43.

Kono M, Nakamura Y, Suda T, Kato M, Kaida Y, Hashimoto D, et al. Plasma CCN2 (connective tissue growth factor; CTGF) is a potential biomarker in idiopathic pulmonary fibrosis (IPF). Clin Chim Acta 2011;412:2211-15.

Lipson KE, Wong C, Teng Y, Spong S. CTGF is a central mediator of tissue remodeling and fibrosis and its inhibition can reverse the process of fibrosis. Fibrogenesis Tissue Repair 2012;5:S24.

Mori R, Kondo T, Ohshima T, Ishida Y, Mukaida N. Accelerated wound healing in tumor necrosis factor receptor p55-deficient mice with reduced leukocyte infiltration. Faseb J 2002;16:963-74.

Rachfal AW, Brigstock DR. Connective tissue growth factor (CTGF/CCN2) in hepatic fibrosis. Hepatol Res 2003;26:1-9.

Sisco M, Kryger ZB, O'Shaughnessy KD, Kim PS, Schultz GS, Ding XZ, et al. Antisense inhibition of connective tissue growth factor (CTGF/CCN2) mRNA limits hypertrophic scarring without affecting wound healing in vivo. Wound Repair Regen 2008;16:661-73.

Soutschek J, Akinc A, Bramlage B, Charisse K, Constien R, Donoghue M, et al. Therapeutic silencing of an endogenous gene by systemic administration of modified siRNAs. Nature 2004;432:173-78.

Spitzer S, Eckstein F. Inhibition of deoxyribonucleases by phosphorothioate groups in oligodeoxyribonucleotides. Nucleic Acids Res 1988;16:11691-704.

Suvik A, Effendy A. The use of modified Masson's trichrome staining in collagen evaluation in wound healing study. Mal J Vet Res 2012;3:39-47.

Thierry AR, Dritschilo A. Intracellular availability of unmodified, phosphorothioated and liposomally encapsulated oligodeoxynucleotides for antisense activity. Nucleic Acids Res 1992;20:5691-98.

Wang Q, Usinger W, Nichols B, Gray J, Xu L, Seeley TW, et al. Cooperative interaction of CTGF and TGF-beta in animal models of fibrotic disease. Fibrogenesis Tissue Repair 2011;4:4.

Wolfrum C, Shi S, Jayaprakash KN, Jayaraman M, Wang G, Pandey RK, et al. Mechanisms and optimization of in vivo delivery of lipophilic siRNAs. Nat Biotechnol 2007;25:1149-57.

Woolf TM, Jennings CG, Rebagliati M, Melton DA. The stability, toxicity and effectiveness of unmodified and phosphorothioate antisense oligodeoxynucleotides in Xenopus oocytes and embryos. Nucleic Acids Res 1990;18:1763-69.

Zhao Q, Matson S, Herrera CJ, Fisher E, Yu H, Krieg AM. Comparison of cellular binding and uptake of antisense phosphodiester, phosphorothioate, and mixed phosphorothioate and methylphosphonate oligonucleotides. Antisense Res Dev 1993;3:53-66.

## FIGURE LEGENDS

**Figure 1. Structure and gene silencing activity of cp-asiRNA targeting CTGF** (a) Schematic presentation of cp-asiRNA targeting CTGF (cp-asiCTGF). Red character: 2'-O-Methyl modification, asterisk: phosphorothioate modification, chol.: cholesterol (b) Repression of CTGF mRNA expression by siCTGF, asiCTGF or cp-asiCTGF in A549 cells. The A549 cells were either transfected or incubated with CTGF targeting siRNAs for 24 hours and the level of target mRNA was analyzed by quantitative real-time PCR (qPCR). The CTGF levels were normalized to GAPDH levels. (c) Repression of CTGF mRNA expression level by cp-asiCTGF in A549 cells. The A549 cells were incubated with different concentration of cp-asiCTGF for 24 hours and dose-dependent level of CTGF mRNA was analyzed by quantitative real-time PCR (qPCR). All data in the bar graph represent the mean ±SD values of three independent experiments. Transfection: siRNA transfection, Treatment: siRNA treatment without transfection reagent, NT: no treatment control.

**Figure 2. *In vitro* analysis of cp-asiCTGF target gene silencing activity**. (a, b) Expression of CTGF protein (a) and mRNA (b) after cp-asiCTGF treatment. cp-asiCTGF was treated into different cell lines (A549, HeLa, and HaCaT) for 48 hours. For protein level analysis, cell lysates were extracted and the extracts were resolved by 12% SDS-PAGE. CTGF antibody was used to detect CTGF protein. β-Actin was used as the control. Bands from western blots were quantified and normalized by the ImageJ and presented as bar graph representing the ratio of band intensities relative to that of the control sample (n = 3). mRNA level analysis was conducted as described in figure 1. (c) Target protein knockdown by cp-asiCTGF treatment in human keloid fibroblasts (KEL FIB). KEL FIB cells were transfected or treated with cp-asiCTGF for 48 hours. Whole cell lysates were isolated and western blot analysis was performed as described in panel

(a). GAPDH was used as the control. All data in the bar graph represent the mean ±SD values of three independent experiments. KEL FIB: Keloid fibroblasts cells. *$P$<0.5 compared to control (TGF-β induction without cp-asiCTGF treatment for panel a and b, no cp-asiCTGF treatment for panel c).

**Figure 3. *In vivo* analysis of cp-asiCTGF.** (a) Repression of target mRNA by cp-asiCTGF in rat skin. Rat skin was treated with cp-asiCTGF or SC cp-asiCTGF (cp-asiRNA with scrambled sequence used as negative control) through intradermal injection (1, 0.7, 0.4, and 0.1mg per injection). 24 hours later, total RNA extracted from the skin of treated rats (n = 3) was reverse transcribed and CTGF mRNA levels were quantified by qPCR. The rat CTGF levels were normalized to GAPDH levels. All data in the graph represent the mean ±SD values of three independent experiments. (b) Western blot analysis of rat skin treated with cp-asiCTGF or SC cp-asiCTGF (1 mg per injection) for 72 hours. GAPDH is shown as a loading control. Bands from western blots were quantified and normalized by the ImageJ and presented as bar graph representing the ratio of band intensities relative to that of the control sample (n = 3). (c) Laser scanning confocal microscopy analysis of cp-asiCTGF distribution in rat skin. 6 hours after intradermal injection of Cy5.5 labeled cp-asiCTGF (100 μl from 0.1 mg/ml solution), rat skin at injection site was collected and processed for confocal scanning laser microscopy analysis. Red signal represents Cy5.5 and blue signal represents 4', 6-diamidino-2-phenylindole (DAPI). Scale bar = 1 mm. Untreated: Normal untreated skin control, cp-asiCTGF: cp-asiCTGF injection, SC cp-asiCTGF: SC cp-asiCTGF injection. **$P$<0.01 compared to the untreated skin sample.

**Figure 4. Analysis of cp-asiCTGF activity in excision rat skin wound model.** 1.5 mg of cp-asiCTGF or SC cp-asiCTGF was injected on days 14, 18, 22 and 26 after the excision wound. Rat scar skin was harvested on day 29. (a-c) mRNA level analysis of fibrosis factors including CTGF,

collagen type I, and collagen type III. mRNA level of each gene on day 29 was measured by qPCR as described in figure 3. Box and whisker plots: horizontal line, median; box, 25th and 75th percentiles; whiskers, min and max. (d) Western blot of rat skin scar on day 29. β-Actin is used as loading control. (e) Quantification of band intensities from the western blot is presented as bar graph representing the mean ±SD values (n = 4). Untreated: Normal uninjured skin control. Saline: Vehicle injection control, cp-asiCTGF: cp-asiCTGF injection, SC cp-asiCTGF: SC cp-asiCTGF injection. ***$P$<0.001, **$P$<0.01, *$P$<0.05 compared to the saline injected sample.

**Figure 5. Histological analysis of excision wound in rat skin.** (a-f) Localization of CTGF (a, b, c) and collagen type I (d, e, f) protein was determined by immunohistochemistry on day 29. Scale bar = 100 μm. (g-i) Collagen deposition represented through Masson's trichrome staining on day 29. Scale bar = 1 mm. The arrow indicates excision site of rat skin surrounded by dotted line. (j-l) Quantification of immunohistochemistry and Masson's trichrome staining data in panel (a-i). Bar indicates mean ±SD (n = 3). Saline: Vehicle injection control, cp-asiCTGF: cp-asiCTGF injection, SC cp-asiCTGF: SC cp-asiCTGF injection. *$P$<0.05 compared to the saline injected sample.

Figure 1.

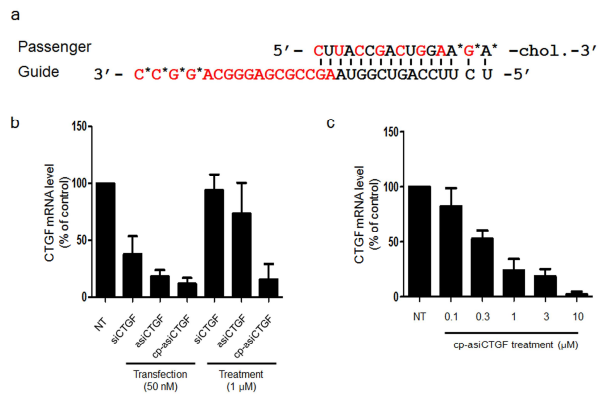

Figure 2.

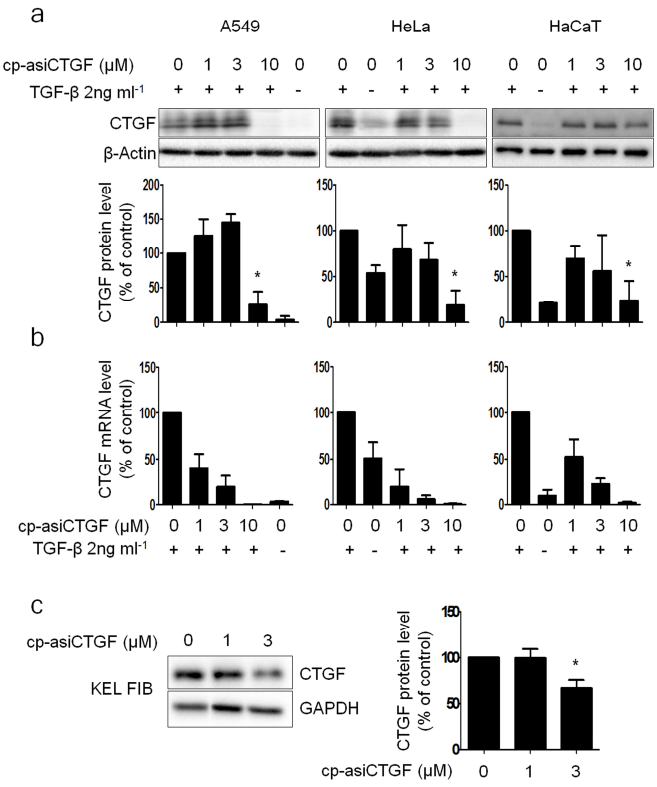

Figure 3.

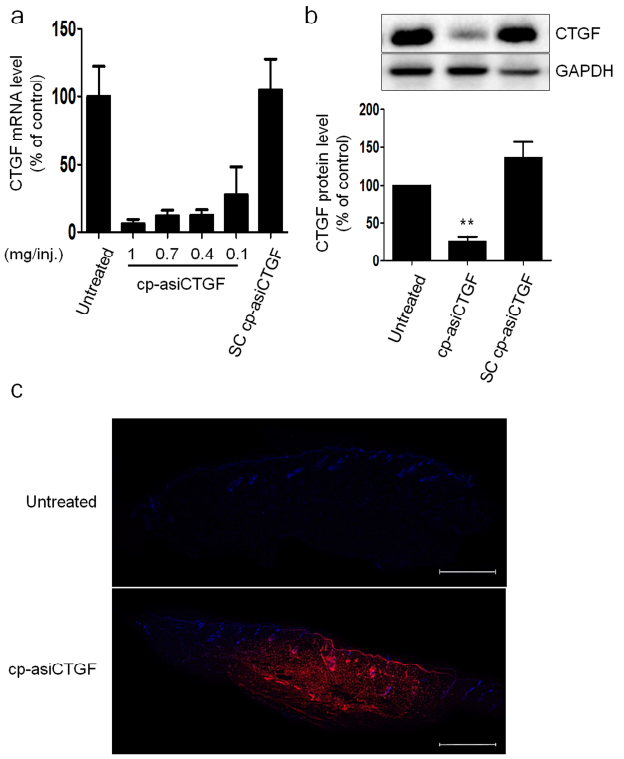

Figure 4.

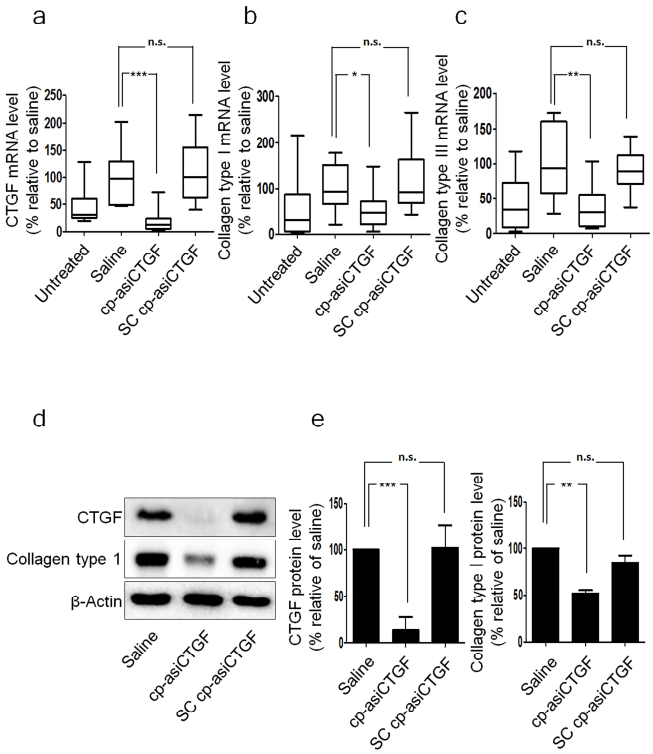

Figure 5.